Three dimensional discrete element simulation of trapdoor unloading and gravity flow of sandy granular material

Simulation tridimensionnelle par les éléments distincts du débit de décharge et d'écoulement gravitaire du matériau granulaire sableux

Kikkawa N., Itoh K., Toyosawa Y.
National Institute of Occupational Safety and Health, Japan

Pender M.J., Orense R.P.
University of Auckland, New Zealand

ABSTRACT: Reported herein are numerical simulations, using the discrete element method (DEM), of a bed of granular material having a moveable trapdoor over part of the underlying boundary. Kikumoto & Kishida 2003, and Kikumoto et al. 2003 measured the vertical stresses on a trapdoor and the adjacent boundaries in tests in which Toyoura sand was used to represent natural ground. The DEM simulation modelled well the vertical stress measured on the trapdoor when it was moved downward and also the vertical stresses on the boundaries adjacent to the trapdoor. Next the gravity flow of the sand was calculated when the trapdoor was suddenly removed; it was found that there was a complex dynamic response in the vertical stress on the boundary immediately adjacent to the opening created, but only modest changes further away. The motivation for these DEM simulations was the desire to understand better the processes involved in tunnel construction when there is a partial collapse of the face or the roof near the tunnel face. Although safety in the excavation of underground openings has improved markedly in recent decades, accident statistics for this type of work remain a challenge for the Japanese construction industry.

RÉSUMÉ: On présente ici des simulations numériques, à l'aide de la méthode d'éléments distincts (DEM), d'un lit de matériau granulaire ayant une trappe amovible sur une partie de la limite sous-jacente. Kikumoto & Kishida 2003, Kikumoto et al., 2003 ont mesuré les contraintes verticales sur une trappe et ses frontières adjacentes dans les essais où le sable de Tayoura a été utilisé pour représenter le terrain naturel. La simulation par DEM modélise bien la contrainte verticale mesurée sur la trappe quand il a été déplacé vers le bas et aussi les contraintes verticales sur les frontières adjacentes à la trappe. Ensuite, l'écoulement par gravité du sable a été modélisé lorsque la trappe a été soudainement retirée. Il a été constaté qu'il y avait une réponse dynamique complexe de la contrainte verticale sur la limite juste à côté de l'ouverture créée, mais seulement de légères modifications plus loin. La motivation pour ces simulations de DEM a été de mieux comprendre les processus impliqués dans la construction de tunnels lorsqu'il y a un effondrement partiel de la face ou sur les cotés près du front du tunnel. Bien que la sécurité dans l'excavation des cavités souterraines se soit nettement améliorée au cours des dernières décennies, les risques d'accidents dans ce type d'opération demeurent un défi pour l'industrie de la construction japonaise.

KEYWORDS: tunnel, trapdoor, gravity flow, discrete element method, sand

1 INTRODUCTION

At present, almost all mountain tunnels constructed in Japan are excavated utilizing the New Austrian Tunneling Method (NATM). This tunneling method was advocated by Prof. Rabcewicz from Austria in 1964 (Rabcewicz 1964a, b, 1965). In Japan, the method has been applied to tunnel construction since about 1978. On the other hand, tunnels in cities are often excavated utilizing a Shield Tunneling Method. Since adopting these methods there has been a substantial decrease in the number of accidents and fatalities in tunnel construction in Japan. However, there is still a relatively higher incidence of accidents during tunnel construction than in the construction industry in general. In tunnel construction, rock fall events in rocky ground and partial collapse from the roof and face in sandy ground are characteristic of the types of accident that occur.

Rock falls and the partial collapse at the face induce stress redistribution. This in turn leads to the formation of a ground arch above the failed roofs with accompanying local stress increases at the foot of the arch. These increased stresses may cause the collapse to extend to the whole tunnel itself. This mode of failure is more likely in sandy ground. Therefore, when minor to modest collapse occurs it is very important to know how much the stress at the foot of the ground arch will increase above the values prior to the collapse.

The stress redistribution induced by lowering of a trapdoor has been tested and analysed (Terzaghi 1936, Murayama & Matsuoka 1971, Kikumoto & Kishida 2003, Costa et al 2009 etc.). Murayama & Matsuoka (1971) and Kikumoto & Kishida (2003) measured the earth pressure on the trapdoor and the surroundings during the lowering of the trapdoor. The Kikumoto & Kishida (2003) data are compared with the results from DEM modelling herein. Costa et al (2009) investigated the ground deformation mechanisms during lowering of a trapdoor with various ratios of the sand layer depth to the width of the trapdoor. They showed when the ratio is low, so modelling a shallow tunnel, the zone failure is limited to sand adjacent to and above the trapdoor. On the other hand, when the ratio is high, which represents a deep tunnel, the failure region is more widely spread beyond the width of trapdoor.

Earth pressure increases during a gravity flow were analysed using a two dimensional DEM by Kiyama & Fujimura 1983. They concluded that the earth pressure on the foot of the ground arch during the gravity flow is much higher than the static earth pressure. This finding is confirmed by the results of the DEM modeling presented in this paper.

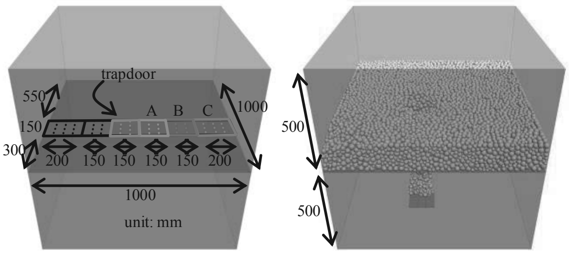

Figure 1. Trap door and gravity flow testing apparatus (left), and DEM simulation (right).

In this study, we used a 3D particle flow code (PFC3D, Itasca 2012) to perform discrete element (DEM) simulations of the trapdoor experiments reported by Kikumoto & Kishida 2003, Kikumoto et al. 2003. In this work a bed of Toyoura sand 75~300 mm deep was placed by air pluviation into a box one metre square. The relative density of Toyoura sand achieved by this method was about D_r= 88%. Along the middle floor of the box, an instrumented strip 150 mm wide had been installed so that the vertical stress distribution could be measured. One part of this strip formed the trapdoor which could be moved downwards in a controlled manner or removed. With this arrangement the vertical stresses on the trapdoor and the floor of the container adjacent to the trapdoor could be monitored. These details are shown in the left hand side of Figure 1.

The first part of the DEM simulation calculated the vertical stress on the trapdoor and floor of the box as the trapdoor was moved downwards at a constant rate. In the second part of the simulation the vertical stresses on the floor of the container were calculated during gravity flow of the sand from the container after the sudden removal of the trapdoor.

2 OUTLINE OF DEM MODELLING OF THE TRAPDOOR AND GRAVITY FLOW TESTS

2.1 *Three-dimensional Trapdoor and Gravity Flow Tests*

The right hand side of Figure 1 shows the configuration of the DEM model. The dimensions of the soil container are almost the same as the experimental testing apparatus used by Kikumoto & Kishida 2003, except the depth of the sand layer is 150 mm whilst Kikumoto et al used various depths between 75 and 300 mm.

2.2 *DEM analysis*

Kikumoto & Kishida 2003 used Toyoura sand (D_{50}= 0.20mm at D_r= 88%) in the experimental trapdoor tests. For the DEM analysis it is difficult to simulate the grain size distribution, particle shapes, and other properties of the sand. In this study, we used spherical particles for the DEM analysis, and calculated the normal and tangential stiffness coefficients, k^n, k^s, using P- and S-wave velocities that had been measured for Toyoura sand by Hori et al 2010. The stiffness coefficients are obtained from:

$$k^n = \frac{\pi R \rho_s V_p^2}{3} \quad (1)$$

$$k^s = \frac{\pi R \rho_s V_s^2}{3} \quad (2)$$

where: V_p and V_s are respectively the P- and S-wave velocities of the granular medium , R is the average of sphere radius, ρ_s is the density of spherical particles. It is known that both normal and tangential interparticle stiffnesses may be functions of both wave velocities, but equations (1) and (2) assume that the normal stiffness depends only on V_p and the tangential stiffness only on V_s. Values for V_p and V_s of Toyoura sand of 403 and 254 m/sec respectively were obtained by Hori et al 2010 using the bender and extender element tests; thus k^n and k^s were calculated to be 4.7 × 10^6 and 1.9 × 10^6 N/m, respectively. Table 1 shows the DEM parameters used in this study.

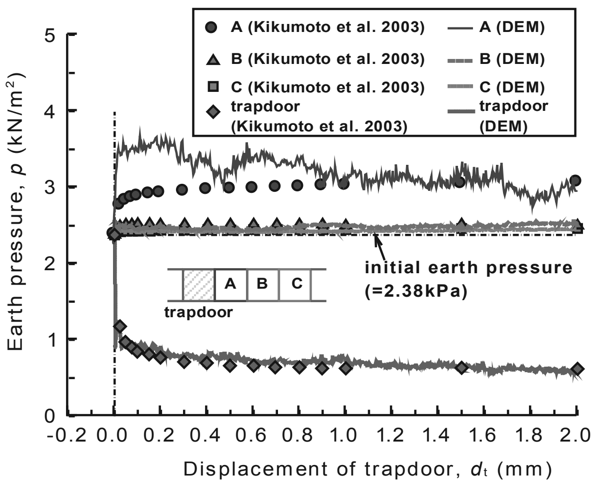

Figure 2. Vertical stresses on the trapdoor and the floor next to the trapdoor against trapdoor displacement.

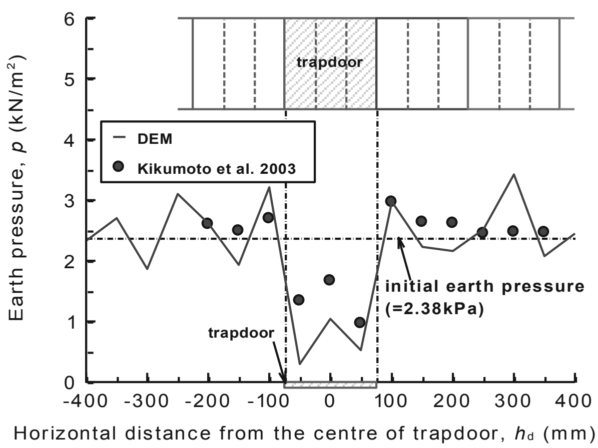

Figure 3. Experimental and DEM distributions of vertical stress at a trapdoor displacement of 2.0mm, with an overburden depth of 150 mm.

Table 1. DEM parameters used in this study

Parameter	Symbol	Value	Unit
Density of sphere	ρ_s	2650	kg/m^3
Mean radius of sphere	R	10.5	mm
Ratio of maximum and minimum radius of sphere	R_{max}/R_{min}	2.0	-
Normal stiffness	k^n	4.7 × 10^6	N/m
Tangential stiffness	k^s	1.9 × 10^6	N/m
Friction coefficient	μ	0.5	-
Critical damping ratios	β_n, β_s	0.8	-

2.3 *DEM procedure for trapdoor and gravity flow tests*

The DEM procedures for the trapdoor and gravity flow tests are as follows:

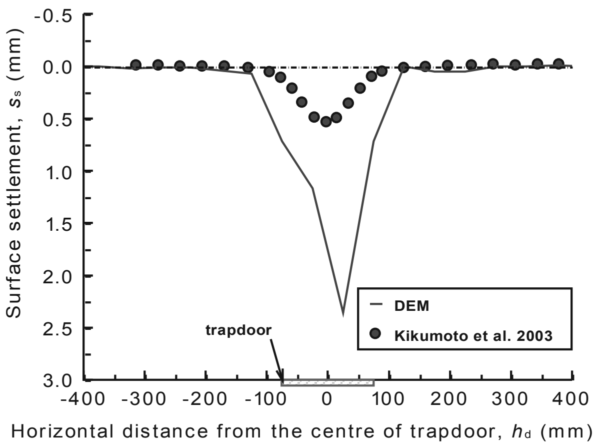

Figure 4. Surface settlement of the sand above the centre of the trapdoor when d_t= 2.0mm, layer thickness 150 mm.

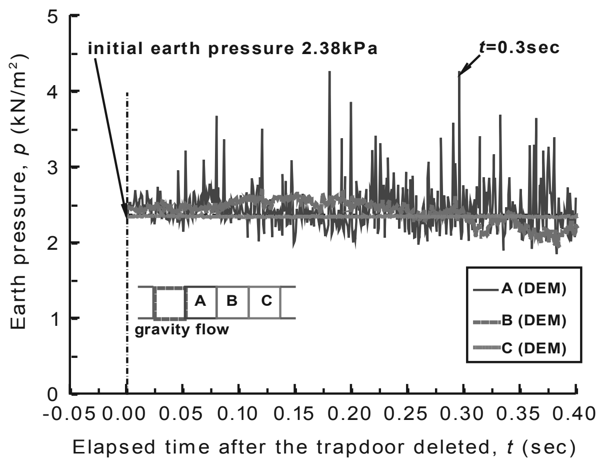

Figure 5. Vertical stress on the floor next to the trapdoor during gravity flow.

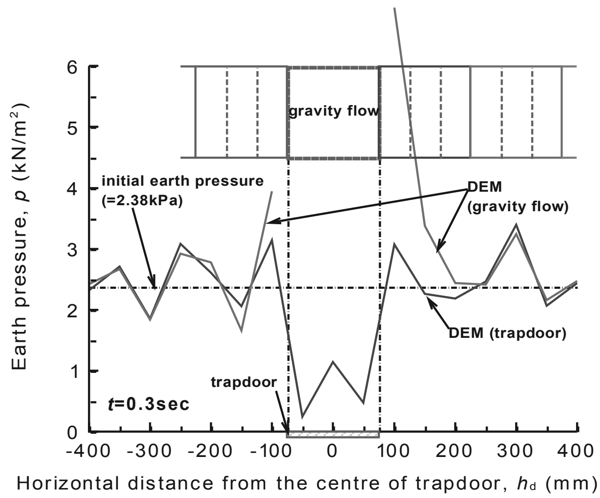

Figure 6. Comparison of vertical stress distributions on the floor next to the trapdoor during trapdoor lowering and during gravity flow at the elapsed time of 0.3sec.

1) Set-up the geometry of the walls and floor of the container and the elements on the floor where the contact stresses will be monitored and the details of the trapdoor as shown on the left hand side Figure 1. The trapdoor is 150 mm long and 150 mm wide and consists of three elements 50 mm long by 150 mm wide. The walls and floor of the container are assumed to be rigid.

   The normal and tangential stiffnesses between the floor elements and the spherical particles are the same as those of between the spherical elements. The friction coefficient between the spherical particles and the floor elements is 0.5, which is the same as that between the particles.
2) Generate the spherical elements above the floor in the upper part of the container to a depth of 150mm. Calculations are repeated under gravity loading until the displacement rates of the spheres approach zero and the bed has come to equilibrium. Knowing the maximum and minimum void ratios of Toyoura sand, the relative density of the sand bed was estimated to be 86%.
3) To simulate the trapdoor tests, the trapdoor was lowered at a constant displacement rate of 5mm/sec. The vertical stresses on the trapdoor and the floor next to the trapdoor were calculated.

   For the gravity flow simulations, the trapdoor was removed instantaneously and dynamic vertical stresses on the floor next to the trapdoor were calculated.

3 RESULTS AND DISCUSSION

First, the experimental data is compared with the DEM analysis data in the trapdoor tests and then the gravity flow simulation is discussed.

3.1 *Trapdoor tests*

Figure 2 shows the variation of vertical stress, p, on the trapdoor against the downward displacement, d_t, and on the floor elements adjacent to the trapdoor. The depth of the sand layer was 150 mm, equal to the width of the trapdoor; the initial vertical pressure on the floor of the container was 2.38kN/m^2. The plots compare the experimental data obtained by Kikumoto et al (2003) with the calculated DEM values. The centre of elements A, B and C are respectively 150mm, 300mm and 450mm from the centre of the trapdoor. It is seen that the vertical stress adjacent to the trapdoor is affected by the trapdoor movement but further away the influence of the movement is negligible. The vertical stress on the trapdoor rapidly decreased at the onset of the downward movement, and the experimental and DEM values corresponded well. The final value when d_t= 2.0mm is 0.62kN/m^2 for the DEM results. On the other hand, the vertical stress on element A increased rapidly with the lowering of the trapdoor and then settles to a constant value of 3.0kN/m^2 in the DEM. The initial rate of increase for the vertical stress for element A in the DEM results is different from that of the experimental data. This reason is not clear, but it may be related to the difference in dilation rate between Toyoura sand and spherical DEM elements.

The vertical stresses on floor elements B and C increased slightly and there is good agreement between the experimental data and the calculated DEM results.

Figure 3 shows the distribution of vertical stress laterally from the centre of the trapdoor when d_t= 2.0mm. The vertical stress on the trapdoor decreased and increased on the floor next to the trapdoor. The DEM data show a sawtooth distribution not seen in the experimental data.

Figure 4 shows the surface settlement of the sand above the centre of the trapdoor when d_t= 2.0mm at the depth of the sand layer was 150 mm. The experimental data was measured by the laser displacement scanner which accuracy was 1μm (Kikumoto et al. 2003). It is, however, Figure 4 that reveals the most significant shortcoming of the DEM modelling as the experimental and calculated subsidence trough at the upper surface of the sand are very different; the surface settlement in the experimental test is much smaller than that from the DEM modelling. Again this could be caused by differences in dilatancy between the Toyoura sand and the spherical DEM elements. The particle shape of the Toyoura sand is well known to be sub-angular, so that in Toyoura sand it may be possible to establish the ground arch even in a loose density state. On the other hand, the spherical particles, even at the close packing achieved in the numerical simulations, may not establish an effective ground arch, so that the effect of the settlement of the trapdoor could propagate up through the sand layer to the surface above.

Here, we have verified that the earth pressure on the trapdoor and the surroundings could be modelled using DEM methods. On the other hand, the surface settlement could not be evaluated using a simple calculation in the DEM analysis. In near future, we would like to extend the DEM modelling to include the stabilisation of the tunnel face using shotcrete, rock-bolts, and steel arch supports and also improve the modelling of ground surface settlement.

3.2 *Gravity flow tests*

The above confirms that the DEM analysis expresses well the vertical stress as the trapdoor lowered; although the settlement of the surface of the sand above the trapdoor is least satisfactorily modeled. Here, we wish to investigate the distribution of the vertical stress on the floor adjacent to the position of the trapdoor during the gravity flow following the deletion of the trapdoor. This might give some insight into the processes following a small collapse of a part of the roof of a tunnel. After small collapse, the stresses at the foot of the ground arch may increase to such an extent that total collapse occurs.

Figure 5 shows the vertical stress against elapsed time after the trapdoor was removed. The elapsed time of 0.4sec corresponds with the displacement of the trapdoor of 2.0mm in the Figure 2. The vertical stress at element A undergoes a rapid cyclic variation suggesting that in the DEM simulations the establishment of the ground arch is a complex dynamic process rather than a static one. The vertical stresses on elements B and C were not much changed from the initial vertical stress calculated when the bed of spherical particles had come to equilibrium.

Figure 6 shows the vertical stress against the horizontal distance from the centre of the trapdoor at an elapsed time of 0.3sec after the trapdoor was removed. The elapsed time of 0.3sec corresponds with the displacement of the trapdoor of 1.5mm in the Figure 2. Note that the vertical stress at element A, just next to the trapdoor during gravity flow was 2.26 times that calculated at the displacement of the trapdoor of 1.5mm when the trapdoor was lowered at a steady rate. This is evidence of the increased stresses at the foot of the ground arch mentioned in the Introduction.

3.3 *Implications for tunnel construction*

With regard to tunnel construction it is possible to draw two conclusions from the experiments of Kikumoto et al (2003) and the DEM modeling discussed in this paper. First, the steady lowering of the trapdoor indicates that yielding of parts of a tunnel lining system is unlikely to generate large increases in loading on adjacent parts of the lining. Second, sudden collapses of part of the tunnel face may induce dynamic effects which lead to large increases in loads on other parts of the system. This in turn provides some indication for the effectiveness of the New Austrian Tunnelling Method, that is the immediate placement of support provided by the NATM even before it is fully stiffened, is effective because it prevents even partial collapses.

4 CONCLUSIONS

We performed DEM analysis of a bed of sand modeled using spherical particles in order to investigate how the distribution of the vertical stress on the supporting lower boundary of the sand container changed during steady lowering of the trapdoor and during gravity flow following the sudden removal of the trapdoor. The summary of the results obtained from this work is as follows:

1) The DEM analysis modeled well the changes in vertical stress during lowering of the trapdoor, Figures 2 and 3.
2) The DEM calculated settlement of the surface of the sand above the trapdoor severely over-predicted the experimentally observed values, Figure 4. Our suggested explanation for this difference is that the relatively large spherical particles used in the DEM modeling do not represent adequately the dilatancy properties of Toyoura sand.
3) During gravity flow, after the sudden removal of the trapdoor, the vertical stress on the floor immediately adjacent showed a complex dynamic variation. With increasing lateral distance from the opening this variation was much less significant, Figure 5.
4) The maximum vertical stresses on the floor next to the opening, after the sudden removal of the trapdoor, were several times larger than the maxima when the trapdoor was lowered at a steady rate, Figure 6.
5) In both the steady lowering of the trapdoor and the gravity flow after the sudden removal, the lateral distribution of the vertical stress on the floor calculated with the DEM software exhibited a saw-tooth variation (Figures 3 and 6).

The implications of this DEM modelling for tunnel construction is that even a yielding support system, such as shotcreting applied to a tunnel heading immediately after excavation, is very significant because it protects against large dynamic pressure that could be induced during a partial collapse.

5 REFERENCES

Costa, Y. D., Zornberg, J. G., Bueno B. S. and Costa C. L. 2009. Failure mechanisms in sand over a deep active trapdoor, *Journal of Geotechnical and Geoenvironmental Engineering*, ASCE, 1741-1753.

Hori, T., Kikkawa, N., Okita, T. and Mitachi, T. 2010. Measurement of S-wave and P-wave velocities by Bender Element tests, *Proc. of the 6th conference of the Kanto Branch of the Japanese Geotechnical Society (GeoKanto2010)*, 4p (in Japanese).

Itasca Consulting Group Inc. 2012. Particle Flow Code in 3 Dimensions Theory and Background.

Kikumoto, M. & Kishida, K. 2003. Mechanical behavior on the sandy ground through the 3-D trapdoor experiment, *Proc. of the 12th Asian Regional Conference on Soil Mechanics & Geotechnical Engineering*, 4p.

Kikumoto, M., Kimura, M., Kishida, K. and Adachi, T. 2003. Three dimensional trapdoor experiments and its numerical analyses on the mechanical behavior during tunnel excavation, *Journal of Geotechnical Engineering* (III), Journal of Japan Society of Civil Engineers, Vol. 65, No. 750, 145-158 (in Japanese).

Kiyama H. and Fujimura H. 1983. Application of Cundall's discrete block method to gravity flow analysis of rock-like granular materials, *Journal of Japan Society of Civil Engineers*, No. 187, pp. 95-108 (in Japanese).

Murayama S. and Matsuoka H. 1971. Earth pressure on tunnels in sandy ground, *Journal of Japan Society of Civil Engineers*, No. 333, pp. 137-146 (in Japanese).

Rabcewicz, L. V. 1964a, b, 1965. The New Austrian Tunneling Method, part one, two and three, *Water Power*, November, December and January, 453-457, 511-515 and 19-24.

Terzaghi, K. 1936. Stress distribution in dry and saturated sand above a yielding trap-door, *Proc. 1st International Conference on Soil Mechanics and Foundation Engineering*, Cambridge, Mass., 35-39.